J|A|C|S
ARTICLES
Published on Web 11/13/2002

Density Functional Theory Study of Enantiospecific Adsorption at Chiral Surfaces

Željko Šljivančanin,[†,‡,||] Kurt V. Gothelf,[†,§] and Bjørk Hammer*[,†,‡]

Contribution from the Interdisciplinary Nanoscience Center (iNANO), Institute of Physics and Astronomy, and Center for Catalysis, Department of Chemistry, University of Aarhus, DK-8000 Aarhus C, Denmark

Received June 10, 2002

Abstract: Density functional theory calculations are carried out for the adsorption of a chiral molecule, (*S*)- and (*R*)-$HSCH_2CHNH_2CH_2P(CH_3)_2$, on a chiral surface, Au(17 11 9)^S. The *S*-enantiomer is found to bind more strongly than the *R*-enantiomer by 8.8 kJ/mol, evidencing that the chiral nature of the kink sites at the Au(17 11 9) surface leads to enantiospecific binding. The adsorption of two related chiral molecules, $HSCH_2CHNH_2COOH$ ("cysteine") and $HSCH_2CHNH_2CH_2NH_2$, does not, however, lead to enantiospecific binding. The results of the density functional calculations are broken down into a local binding model in which each of the chiral molecule's three contact points with the surface provides a contribution to the overall adsorption bond strength. The enantiospecific binding is demonstrated to originate from the simultaneous optimization of these three *local* bonds. In the model, the deformation energy costs of both the molecule and the surface are further included. The model reveals that the molecule may undergo large deformations in the attempt to optimize the three bonds, while the surface deforms to a lesser extent. The most favorable binding configurations of each enantiomer are, however, characterized by small deformation energies only, justifying a local binding picture.

1. Introduction

Enantioselective reactions and interactions occur at many levels ranging from enzymatic processes in living organisms to various types of enantiocontrol in industry and research laboratories. Since it has become clear that a majority of chiral drugs can be administrated safely only in the enantiomerically pure form, the industrial need for new asymmetric methods has powered the current level of research in this area.[1] Asymmetric catalysis is one of the most promising approaches for the synthesis of optically active molecules.[2] The major focus of asymmetric catalysis has been on homogeneous or polymer supported catalysts,[2−4] while to the best of our knowledge no reports on asymmetric catalysis by chiral metal surfaces have appeared so far. The existence of chiral surfaces for the FCC crystal structure taken by most of the late transition and noble metals relevant for catalysis was pointed out only recently by Gellman and co-workers.[5] Since then, an intense research effort has been aimed at understanding and controlling the possible role of such chiral surfaces for enantioselective heterogeneous catalysis.

The first experiments to be conducted in the field were for the two chiral forms of a silver surface, Ag(643)^R and Ag(643)^S, but no enantioselectivity was found either in the desorption characteristics of (*R*)- and (*S*)-butan-2-ol or in the reaction rate toward β-hydride elimination for (*R*)- and (*S*)-butane-2-oxide.[5] Subsequent theoretical investigations by Sholl[6] of the adsorption configurations and binding energies of (*R*)- and (*S*)-limonene and (*R*)- and (*S*)-1,2-dimethylcyclopropane at Pt(532)^S, Pt(643)^S, and Pt(754)^S surfaces predicted, however, that, for certain systems, enantiospecific binding energy shifts in the order of 2 kcal/mol should be present, which would be within reach for detection. Meanwhile, more recent experiments have now clearly identified, for example, enantiospecific desorption spectra of *R*-3-methylcyclohexanone and (*R*)- and (*S*)-propylene oxides from Cu(643)^R and Cu(643)^S surfaces[7] and enantiospecific cyclic voltammetric profiles for (*D*)- and (*L*)-glucose over Pt(643)^R and Pt(643)^S surfaces.[8]

Until now, the theoretical investigations of chiral specificity in the adsorption on chiral surfaces have been conducted using an empirical potential for the intramolecular and molecule−surface interactions, while the surfaces have been treated as rigid

* Corresponding author. E-mail: hammer@ifa.au.dk.
† Interdisciplinary Nanoscience Center (iNANO).
‡ Institute of Physics and Astronomy.
§ Center for Catalysis.
|| Present address: IRRMA, Ecublens, CH-1015 Lausanne, Switzerland.

(1) (a) Collins, A. N., Sheldrake, G. N., Crosby, J., Eds. *Chirality in Industry: The Commercial Manufacture and Application of Optically Active Compounds*. John Wiley and Sons: West Sussex, U.K., 1995. (b) Collins, A. N., Sheldrake, G. N., Crosby, J., Eds. *Chirality in Industry II: Development in the Commercial Manufacture and Application of Optically Active Compounds*. John Wiley and Sons: West Sussex, U.K., 1998.
(2) Ojima, I., Ed. *Catalytic Asymmetric Synthesis*, 2nd ed.; John Wiley & Sons: New York, 2000.
(3) (a) Osburn, P. L.; Bergbreiter, D. E. *Prog. Polym. Sci.* **2001**, *26*, 2015−2081. (b) Astruc, D.; Chardac, F. *Chem. Rev.* **2001**, *101*, 2991−3023.
(4) For example, see: (a) Hutchings, G. J. *Chem. Commun.* **1999**, 301−306. (b) Thomas, J. M.; Raja, R. *Chem. Commun.* **2001**, 675−687.
(5) McFadden, C. F.; Cremer, P. S.; Gellman, A. J. *Langmuir* **1996**, *12*, 2483−2487.
(6) Sholl, D. S. *Langmuir* **1998**, *14*, 862−867.
(7) Horvath, J. D.; Gellman, A. J. *J. Am. Chem. Soc.* **2002**, *124*, 2384−2392.
(8) Attard, G. A. *J. Phys. Chem. B* **2001**, *105*, 3158−3167.

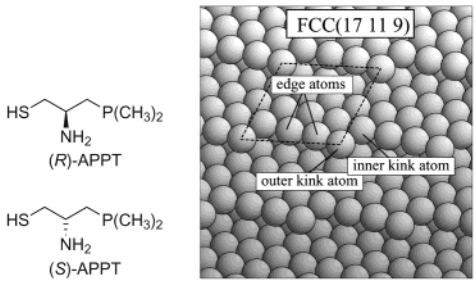

Figure 1. Diagrams of the (*R*)- and (*S*)-APPT enantiomers and a ball model of the Au(17 11 9)^S surface with the (1×1) surface unit cell shown by the dashed line. The surface consists of (111) terraces separated by monatomic steps. The steps have kinks for every four Au atoms. Terrace, inner kink, edge, and outer kink atoms are 9-, 8-, 7-, and 6-fold coordinated to other Au atoms, respectively.

crystals with the metal atoms at truncated bulk positions.[6,9] The use of an empirical potential has obvious advantages in terms of simulation speed and the possibility of including finite temperature effects, but it leaves open questions regarding, for example, the overall accuracy of the computations and the role of substrate relaxations. In recent studies by Sholl and coworkers,[10−12] a step toward a more accurate description was taken by including the metal surface relaxations of the clean surface before the adsorption, as determined by density functional theory calculations. Density functional theory has further been used previously to model chiral adlayers on achiral surfaces.[13−15]

In the present paper, we report the first density functional calculation addressing the adsorption of a chiral molecule on a chiral surface. In the calculations, the adsorbate and metal atoms are treated on an equal footing, allowing for full relaxation of both the molecule and the surface in response to the adsorption process. In our study, we choose to investigate (*S*)- and (*R*)-2-amino-3-(dimethylphosphino)-1-propanethiol (APPT) adsorption on Au(17 11 9)^S. The molecules and the surface are depicted in Figure 1. The choice of functional groups in the molecule is motivated by the previous finding that all of the thiolate, phosphino, and amino groups are able to bind to gold surfaces.[16,17] The propane backbone structure is chosen, since it is capable of hosting these functional groups in a chiral structure.[18] Our DFT calculations show a clear enantiospecific adsorption behavior, which is explained in terms of an enantiospecific dependence of the degree of optimization possible for the three molecule−surface bonds.

2. Computational Method

The density functional theory (DFT) calculations are performed with the DACAPO computer program[19] using the repeated slab approach[20] and the ultrasoft pseudopotential approximation[21] with a plane wave basis set for the Kohn−Sham one-electron wave functions. The chiral Au(17 11 9)^S surface is realized by a super cell containing 36 Au atoms arranged as three sheets of close packed Au atoms forming slabs separated by ∼12 Å of vacuum. The relaxed surface structure before adsorption is shown in Figure 1, which also labels some gold atoms. In this structure, the lower two sheets of close packed Au atoms are kept at their truncated bulk positions using the theoretical lattice constant 4.18 Å, thereby providing the proper boundary conditions for the surface layers and avoiding the spurious strain effects that would result from using the experimental lattice constant (4.08 Å). Whenever adsorbates are introduced, the primitive (1×1) surface unit cell is used, ensuring that adsorbates in adjacent cells are always separated by 3.75 Å or more. For gas-phase molecules we calculate such a separation to cause intermolecular interactions to affect the present results by less than 3 kJ/mol. The basis set contains plane waves with kinetic energies up to 25 Ry and with allowed Bloch wave vectors at a (2×2) grid spanning the first surface Brillouin zone. The electronic exchange−correlation interactions are described using the generalized gradient approximation (GGA) in the revised Perdew−Burke−Ernzerhof (RPBE) functional form[19] for both the structural optimization and the reported energetics. This functional has been shown to give accurate results for the adsorption of atoms and molecules at metal surfaces and for the description of the binding energy of small organic molecules.[22] While absolute adsorption energies calculated with the present method are believed to be converged to the 25 kJ/mol level[19] (the use of a finite number of Au(111) layers in the slab, for example, causes errors at the 10 kJ/mol level[23]) we shall report and interpret even smaller adsorption energy differences, since relative energies are typically more reliable than absolute energies.

Since the adsorbate considered is a thiolate radical, RS$^\bullet$ (with R = $CH_2CHNH_2CH_2P(CH_3)_2$), while its gas phase form is that of a thiol, RSH, the adsorption potential energies reported are obtained as

$$E_{ads}(\mathrm{RS}) = E_{tot}(\mathrm{RS}^\bullet + \mathrm{surf}) - E_{tot}(\mathrm{surf}) - \left\{E_{tot}(\mathrm{RSH}) - \frac{1}{2}E_{tot}(\mathrm{H_2})\right\} \quad (1)$$

where the terms on the right-hand side are the total energies of the fully relaxed system of the adsorbate on the surface, of the fully relaxed, clean surface, of the hydrogenated adsorbate in the gas phase, and of (half) the hydrogen molecule, respectively. In the analysis of the results, we further compute adsorption potential energies of HS$^\bullet$ by setting R = H in eq 1 and of adsorbates, Y, that are not thiolates using the expression:

$$E_{ads}(\mathrm{Y}) = E_{tot}(\mathrm{Y} + \mathrm{surf}) - E_{tot}(\mathrm{surf}) - E_{tot}(\mathrm{Y}) \quad (2)$$

The adsorption potential energies are equal to minus the adsorption bond energies.

3. Results

The study of the enantiospecific adsorption of (*S*)- and (*R*)-2-amino-3-(dimethylphosphino)-1-propanethiol (APPT) on Au(17 11 9)^S proceeds via an investigation of numerous adsorption configurations. The most stable configurations, S_0 and R_0, found in the calculations for each enantiomer are depicted in Figure 2a,b, and the energetics are reported in Table 1. The adsorption system clearly exhibits enantiospecific

(9) Power, T. D.; Sholl, D. S. *J. Vac. Sci. Technol., A* **1999**, *17*, 1700−1704.
(10) Sholl, D. S.; Asthagiri, A.; Power, T. D. *J. Phys. Chem. B* **2001**, *105*, 4771−4782.
(11) Power, T. D.; Sholl, D. S. *Top. Catal.* **2002**, *18*, 201−208.
(12) Power, T. D.; Asthagiri, A.; Sholl, D. *Langmuir* **2002**, *18*, 3737−3748.
(13) Weckesser, J.; De Vita, A.; Barth, J. V.; Cai, C.; Kern, K. *Phys. Rev. Lett.* **2001**, *87*, 096101-1−096101-4.
(14) Barbosa, L. A. M. M.; Sautet, P. *J. Am. Chem. Soc.* **2001**, *123*, 6639−6648.
(15) Humbolt, V.; Haq, S.; Muryn, C.; Hofer, W. A.; Raval, R. *J. Am. Chem. Soc.* **2002**, *124*, 503−510.
(16) Bain, C. D.; Evall, J.; Whitesides, G. M. *J. Am. Chem. Soc.* **1989**, *111*, 7155−7164.
(17) Kühnle, A.; Linderoth, T. R.; Hammer, B.; Besenbacher, F. *Nature* **2002**, *415*, 891−893.
(18) Griffin, J. H.; Kellogg, R. M. *J. Org. Chem.* **1985**, *50*, 3261−3266.
(19) Hammer, B.; Hansen, L. B.; Nørskov, J. K. *Phys. Rev. B* **1999**, *59*, 7413−7421.
(20) Payne, M. C.; Teter, M. P.; Allan, D. C.; Arias, T. A.; Joannopoulos, J. D. *Rev. Mod. Phys.* **1992**, *64*, 1045−1097.
(21) Vanderbilt, D. *Phys. Rev. B* **1990**, *41*, 7892−7895.
(22) Kurth, S.; Perdew, J. P.; Blaha, P. *Int. J. Quantum Chem.* **1999**, *75* 889−909.
(23) Mavrikakis, M.; Stoltze, P.; Nørskov, J. K. *Catal. Lett.* **2000**, *64*, 101−106.

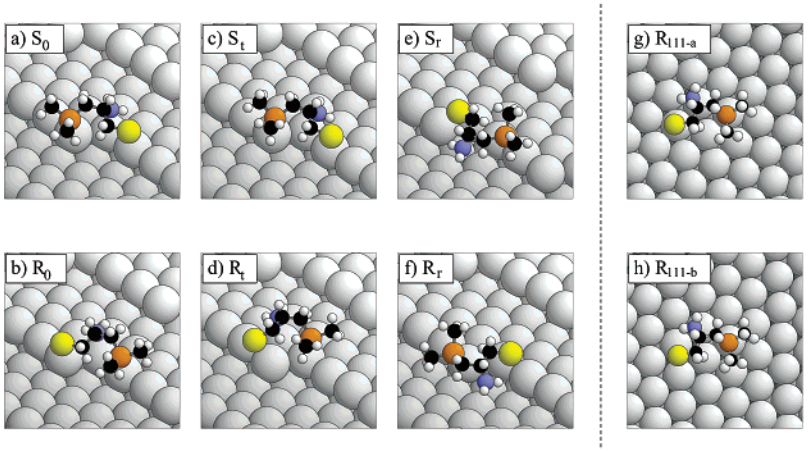

Figure 2. Adsorption configurations for APPT at Au(17 11 9)^S and Au(111) depicted as a ball-and-stick model. Color code: yellow, sulfur; orange, phosphorus; blue, nitrogen; black, carbon; white, hydrogen; gray, gold. (a−f) Chiral Au(17 11 9)^S: S_0 and R_0 are the most stable configurations for each enantiomer. The S_t/R_t and S_r/R_r configurations result from translations along the step edge or rotations around the surface normal of the S_0/R_0 configurations. (g−h) The achiral Au(111) surface: R_{111-a} and R_{111-b} are configurations of (*R*)-APPT adsorbed with the thiol group positioned at either the Au atop or bridge site.

Table 1. Calculated Adsorption Potential Energies (in kJ/mol) for the Entire APPT, E_{ads}(APPT) and for the SH, NH_3, and $PH(CH_3)_2$ Functional Groups, E_{ads}(SH), $E_{ads}(NH_3)$, and $E_{ads}(PH(CH_3)_2)$, Alone Together with the Deformation Energies (in kJ/mol), E_{def}(mol) and E_{def}(surf), for the Molecule and the Surface, Respectively[a]

	E_{ads}(APPT)	E_{model}	E_{ads}(SH)	$E_{ads}(NH_3)$	$E_{ads}(PH(CH_3)_2)$	E_{def}(mol)	E_{def}(surf)
S_0	**−93.1**	−103.1	8.5 (∼−140)	−34.9	*−106.8*	*17.7*	12.4
S_t	−37.4	−33.9	17.1 (∼−135)	−21.3	−90.1	46.3	14.1
S_r	33.5	1.5	−31.7 (∼−180)	6.3	−43.9	56.3	14.5
R_0	**−84.3**	−83.5	−8.8 (∼*−160*)	−31.8	*−75.0*	*17.9*	14.2
R_t	3.8	−8.8	−45.3 (∼*−195*)	−21.0	−38.9	*76.3*	20.1
R_r	10.2	−4.2	−31.2 (∼−180)	−8.8	−73.4	86.3	22.8
R_{111-a}	29.9	19.3	33.8 (∼−120)	−16.4	−47.3	33.8	15.4
R_{111-b}	35.7	13.5	8.7 (∼−140)	−11.6	−48.3	28.0	36.7

[a] The sum of the latter five terms gives the modeled adsorption potential energies, E_{model}, that compare well with E_{ads}(APPT) (cf. Figure 4). The numbers in boldface are the energies of the most stable configurations of each enantiomer. The difference is 8.8 kJ/mol. The thiolate−gold bonds, E_{ads}(SH), appear small in the table, since they were computed according to eq 1, i.e., relative to the RS−H bond in the gas-phase thiol, which is typically of the order 150 kJ/mol. We, therefore, include in parenthesis estimated adsorption bond strengths of the HS−Au bond from the gas-phase HS• radical. These numbers reflect that the HS• adsorption is highly exothermic, while the H_2S + surf → HS/surf + $^1/_2H_2$ reaction is not. Numbers referred to explicitly in the text are written in italic.

behavior with the surface, binding the *S*-enantiomer more strongly by 8.8 kJ/mol than the *R*-enantiomer.

The configurations in Figure 2a,b are the most stable configurations found in an extensive search for the global minimum for each enantiomer, respectively. In Figure 2c−f and Table 1, we show some less stable adsorption configurations that were found for the two enantiomers. These configurations may be thought of as resulting from the S_0 and R_0 configurations by simple geometrical operations followed by relaxation. Specifically, S_t and R_t result from translations of the S_0 and R_0 configurations along the Au step edge, while the S_r and R_r configurations result from ∼180° rotations of the S_0 and R_0 configurations around the surface normal. In all cases, the resulting configurations were fully relaxed after the translation or rotation operations. Configurations in which the adsorbed enantiomers were displaced away from the Au kink site at the step edge, either further along the step edge or onto the Au terraces, were found to be less stable than the configurations S_0 and R_0. Likewise, configurations in which not all three of the thiolate, phosphino, or amino groups were coordinating to gold atoms in the surface were also unfavorable. For comparison, Figure 2g−h shows two configurations, R_{111-a} and R_{111-b}, of (*R*)-APPT adsorbed on Au(111) with the thiol group in either an atop or a bridge position. As revealed by Table 1, these configurations are less bound by more than 100 kJ/mol than, for example, the R_0 configuration.

Inspection of Figure 2a−f reveals that for APPT bound to Au(17 11 9)^S the most stable adsorption configurations found all involve the thiolate or phosphino groups binding to the outer kink Au atom and to the step edge Au atom(s). In addition, the amino group is seen to bind to the Au inner kink atom or to Au atoms in the upper or lower terrace. It thus appears from the calculations that not only is it advantageous for APPT to bind with all three of its functional groups pointing toward the surface, but the positions of the phosphino and thiolate groups are subject to stronger constraints than the position of the amino group. This finding points in the direction that the molecular adsorption configurations may be interpreted as the result of the simultaneous optimization of three *local* bonds between the molecule and the surface.

Conventionally, chemists use a local binding picture for organic molecules. However, at a solid surface, it is not evident that the adsorption of an organic molecule proceeds with uncorrelated local bonds, since, for example, the surface ionic structure may act as a template for the binding. Also, the delocalized nature of the electronic system in the surface may cause correlations in case of incomplete screening. To demonstrate quantitatively that a local binding picture is indeed valid

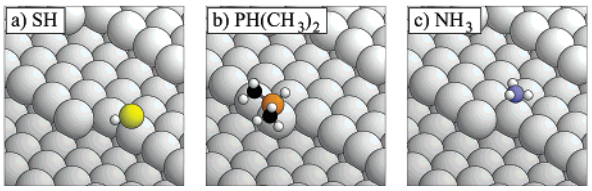

Figure 3. Three individual contact points (bonds) between (*S*)-APPT and the Au(17 11 9)^S surface for the S_0 geometry.

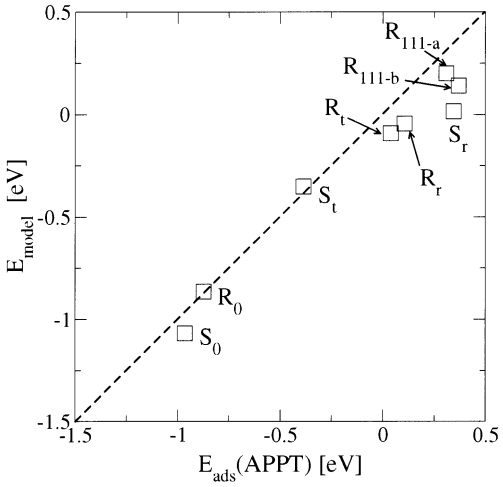

Figure 4. Correlation plot of the total adsorption potential energy, E_{ads}, of the APPT molecule and the modeled adsorption potential energy, E_{model}. The model which is parameter free consists of five additive terms all calculated from density functional theory. The five terms are the adsorption potential energies from each of the three molecule−surface bonds and the deformation energies of the molecule and the surface, respectively. The correlation is particularly favorable for the most stable (i.e., the most important) configurations.

and to extract the individual bond strengths, we proceed by introducing a parameter free model quantity, E_{model}, to be related to the calculated adsorption potential energies:

$$E_{model} = E_{ads}(SH) + E_{ads}(PH(CH_3)_2) + E_{ads}(NH_3) + E_{def}(mol) + E_{def}(surf) \quad (3)$$

Here, the E_{ads}'s are the adsorption potential energies of the thiolate, phosphino, and amino groups alone. These energies are extracted from separate DFT calculations in which one functional group at a time is scissored from the rest of the APPT adsorbate which is replaced with a single hydrogen atom saturating the broken bond. The functional group is kept fixed at the configuration in the adsorbed enantiomer, while the added hydrogen atom is fully relaxed. Figure 3 depicts as an example the three local bonds relevant to the S_0 configuration. The E_{def}'s in the formula are the deformation energies of the molecule and surface alone. These are calculated as minus the relaxation energy of the APPT molecule when the Au surface is removed (the thiolate dangling bond is saturated with a hydrogen atom) and of the surface when the adsorbate is removed.

The calculated DFT values of E_{ads}, E_{def}, and E_{model} are given in Table 1, and Figure 4 presents a correlation plot between the DFT-based adsorption potential energies, E_{ads}(APPT), of the eight configurations of Figure 2 and the modeled adsorption potential energies, E_{model}, based on eq 3. The correlation is quite favorable, in particular for the most important configurations, that is, for the most stable ones. This indeed supports the conception that both the overall magnitude of and the variation in the E_{ads}(APPT) may be discussed on the basis of the individual terms on the right-hand side of eq 3, that is, in terms of the three adsorbate−surface chemical bonds and the deformations of the molecule and the surface required for the formation of these bonds.

4. Discussion

Referring to Table 1, we start by noting that the strongest variations in the local bonds between the APPT functional groups and the Au(17 11 9)^S surface occur for the thiolate−gold and phosphino−gold bonds. Both bonds are rather strong, explaining the possibility of strong variations. The amino−gold interaction is much smaller and hence shows less variation from one structure to the next. We next consider in Table 1 the deformation energies involved for the different configurations. While the surface deformation energies appear small in all cases, the molecular deformation energies are large for all but the most stable configurations, S_0 and R_0. This represents a key finding which allows us to interpret the calculations as follows.

We concentrate our analysis on the thiolate−gold and phosphino−gold bonds, since these were pointed out already as having much larger variations in strengths in our data set compared with the variations in strenght of the amino−gold bond. We consider the following four situations: either (i) the thiolate−gold bond or (ii) the phosphino−gold bond is optimized or (iii) both or (iv) none of the two bonds are optimized. In situation i, the thiolate will be positioned in a bridge site between the outer kink Au atom and a neighboring Au atom as in configuration R_t. The strong thiolate−gold bond here (∼195 kJ/mol) is in accord with the general finding that outer kink atoms are highly reactive[24] and that thiolate prefers bridge binding on gold.[17,25] Table 1, however, reveals (for R_t) that, with the thiolate−gold bond optimized, the molecule must undergo a costly deformation (∼76 kJ/mol) to form the phosphino−gold and amino−gold bonds, rendering this situation unfavorable. The large deformation energies calculated for such structures are the signature that no match of the three functional groups on the adsorbate to three favorable adsorption sites at the surface is readily possible for this configuration.

In situation ii, the phosphorus atom of the phosphino group will be positioned over the outer kink Au atom. This we see as the combined effect of the outer kink atom being the most reactive surface atom and being the most protruding surface atom offering the least steric repulsion for the phosphine methyl groups. Having started from configurations of both *S*- and *R*-enantiomers with an optimized phosphino−gold bond (∼107 kJ/mol), we find according to Table 1 that only for the *S*-enantiomer the thiolate−gold and amino−gold bonds may be formed at a low molecular deformation energy cost (∼18 kJ/mol).

From the discussion of situations i and ii of the individual optimization of the thiolate−gold and phosphino−gold bonds, it is apparent that situation iii of the simultaneous optimization

(24) (a) Hammer, B.; Nielsen, O. H.; Nørskov, J. K. *Catal. Lett.* **1997**, *46*, 31−35. (b) Hammer, B.; Nørskov, J. K. *Adv. Catal.* **2000**, *45*, 71−129. (c) Sljivancanin, Z.; Hammer, B. *Phys. Rev. B* **2002**, *65*, 085414-1−085414-4.

(25) (a) Hayashi, T.; Morikawa, Y.; Nozoye, H. *J. Chem. Phys.* **2001**, *114*, 7615−7621. (b) Vargas, M. C.; Giannozzi, P.; Selloni, A.; Scoles, G. *J. Phys. Chem. B* **2001**, *105*, 9509−9513. (c) Gottschalck. J.; Hammer, B. *J. Chem. Phys.* **2002**, *116*, 784−790. (d) Yourdshahyan, Y.; Rappe, A. M. *J. Chem. Phys.* **2002**, *117*, 825−833.

of the two bonds cannot occur. This is because both bonds preferentially form at the *same* Au site, the outer kink Au atomic site.

Finally, situation iv, in which none of the thiolate−gold or amino-gold bonds are optimized, is to be discussed. This situation is the most difficult for an exhaustive search, but our results show that it is highly relevant. Configurations R_0, R_r, and S_r are thus such situations. In particular, R_0 brings evidence that neither the thiolate−gold nor the phosphino−gold bonds need to be optimized to provide a favorable binding situation. For this configuration, the thiolate is only binding to *one* gold atom despite the known preference for the bridge binding, and the phosphino is binding not to the preferred outer kink Au atom but to a step edge Au atom. The salient feature of this configuration is, however, that strong (S−Au, ∼160 kJ/mol; P−Au, ∼75 kJ/mol), albeit not the strongest possible, bonds are formed at a low molecular deformation energy cost (∼18 kJ/mol).

Comparing now the situations for each enantiomer, we see that the enantiospecific binding comes about because of the spatial mismatch between functional groups and active sites. The degree of mismatch can be estimated from the molecular deformation energies of unfavorable configurations. Only very few configurations are found with strong molecule−surface binding, and among these, the *S*-enantiomer is favored because it may optimize the phosphino−gold bond, while the *R*-enantiomer is less favored, since it optimizes neither the phosphino−gold bond nor the thiolate−gold bond.

The identification of the molecular deformation energy cost originating from the spatial mismatch between the adsorption site template and the position of the adsorbate functional groups can be supported by an inspection of the individual intramolecular bond lengths and bond angles, as listed in Table 2, for gas phase APPT and for adsorbed APPTs. It is seen that while the bond lengths are affected only little by the adsorption, some bond angles are changed significantly. In particular, the $S-C_1-C_2$ bond angle is modified for the S_r, R_t, and R_r configurations that are all associated with large molecular deformation energy costs. The bending of this bond in turn reflects the importance of optimizing the S−Au bond, even at the expense of an intramolecular deformation.

The finding of the enantiospecific adsorption behavior of a chiral molecule forming three bonds to a chiral substrate, in this case to the kink site of a metallic surface, is to be expected from the generic three-point contact model.[26] The three contact points are important because they represent the smallest number of contact points able to discriminate between two different enantiomers. To complement the model, we performed density functional theory calculations with adsorbates different from the APPT molecule. Indeed, we find that if we adsorb the amino acid cysteine, then no enantiospecific adsorption behavior arises,

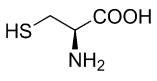

(*R*)-Cysteine

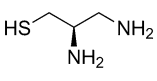

(*R*)-DAPT

since this molecule only binds to the gold surface through its thiolate and amino groups, while the carboxyl group seeks away from the surface. With only two molecule−surface contact points (local bonds), the two enantiomers can bind equally strongly. More surprising, however, are adsorption results we obtain when substituting the carboxyl group of the amino acid with an aminomethylene group to form 2,3-diamino-1-propanethiol (DAPT). The results for the adsorption of the resulting molecule, DAPT, still show no enantiospecific behavior; that is, the energy difference between the adsorption of the two enantiomers is less than k_BT at room temperature, despite the molecule having three groups that all form bonds to the surface. The apparent reason for the lack of enantiospecific behavior for this molecule is that the two amino groups form rather similar bonds to the surface with low molecular deformation energy costs. Only when all three surface−molecule bonds are made dissimilar, in our case by substitution of the carboxyl group of cysteine with a dimethylphosphinomethylene group obtaining thereby the APPT molecule, we find enantiospecific adsorption behavior. The results thus demonstrate that, for the adsorbates considered, the character of the functional groups is most important for the chiral behavior. The results further show that only subtle changes in the binding configurations are responsible for the small energy differences governing the possible enantiospecific adsorption behavior. This means that density functional theory calculations must be conducted in every case studied.

Table 2. Calculated Bond Lengths (Å) and Bond Angles (deg) for the Gas-Phase APPT and the Adsorption Configurations Presented in Figure 2[a]

	S–Au	N–Au	P–Au	$S–C_1$	$N–C_2$	$P–C_3$	$\angle(C_1–C_2–C_3)$
gas-phase APPT				1.84	1.46	1.89	111
S_0	2.43	2.51	2.38	1.84	1.47	1.87	114
S_t	2.43	2.57	2.37	1.84	1.47	1.87	115
S_r	2.53, 2.59	3.04, 3.19	2.47, 3.22	1.86	1.45	1.88	113
R_0	2.38	2.50	2.41	1.84	1.48	1.87	113
R_t	2.46, 2.60	2.56	2.40	1.86	1.47	1.88	113
R_r	2.52, 2.59	2.84	2.33	1.86	1.47	1.86	112
R_{111-a}	2.47	2.49	2.46	1.84	1.47	1.87	115
R_{111-b}	2.56, 2.64	2.68	2.47	1.84	1.46	1.88	113

	$\angle(S–C_1–C_2)$	$\angle(N–C_2–C_1)$	$\angle(N–C_2–C_3)$	$\angle(H–C_2–C_3)$	$\angle(P–C_3–C_2)$
gas-phase APPT	115	110	110	106	119
S_0	113	110	112	105	121
S_t	112	111	109	107	123
S_r	**124**	112	108	105	**126**
R_0	115	110	111	106	121
R_t	**123**	113	111	105	123
R_r	**124**	113	110	105	118
R_{111-a}	115	110	109	107	123
R_{111-b}	116	113	108	106	123

	$\angle(C_2–C_1–H)$	$\angle(N–C_2–H)$	$\angle(P–C_3–H)$
gas-phase APPT	111, 110	113	108, 105
S_0	110, 110	109	106, 105
S_t	109, 111	109	106, 102
S_r	108, 109	111	**102**, 104
R_0	109, 110	109	106, 105
R_t	109, 110	109	106, 103
R_r	108, 110	110	111, 101
R_{111-a}	109, 109	109	104, 105
R_{111-b}	109, 111	110	105, 105

[a] Large deformations of the adsorbed configurations are highlighted in boldface.

(26) (a) Easson, L. H.; Stedman, E. *Biochem. J.* **1933**, *27*, 1257−1266. (b) Booth, T. D.; Wahnon, D.; Wainer, I. W. *Chirality* **1996**, *9*, 96−98.

In conclusion, we have conducted fully relaxed density functional theory calculations of the chiral molecule APPT on a chiral Au(17 11 9)^S surface. We find that the adsorption system is enantiospecific, preferring the adsorption of (*S*)-APPT by 8.8 kJ/mol over the adsorption of (*R*)-APPT. The adsorption site is at the kink site along the monatomic gold step edge. The APPT forms three bonds to the gold surface atoms with its thiolate, phosphino, and amino groups. We successfully reproduce the full density functional results for the adsorption potential energies in terms of a parameter free model involving the individual bond strengths of these three local bonds plus the deformation energies of the molecule and the surface, respectively. The thiolate−gold and phosphino−gold bonds prove most important, showing larger variations in their strengths than the amino-gold bond. We find that, for the *S*-enantiomer, the phosphino−gold bond may be optimized and the remaining bonds may form with fair strengths. For the *R*-enantiomer, however, we find that whether the thiolate−gold or the phosphino−gold bond is optimized, spatial mismatch between functional groups and active sites will obstruct the formation of the remaining bonds. The enantiospecific behavior thus results from the presence of three molecule−surface contact points and the chiral nature of the surface allowing one molecular enantiomer to bind more favorably.

Acknowledgment. Discussions with Angelika Kühnle, Trolle R. Linderoth, and F. Besenbacher are gratefully acknowledged. This work was supported by The Danish Research Councils and the Danish National Research Foundation.

JA027239V